fluids

MDPI

Article

Evaluation of the Adsorption Potential of Benzo(a)pyrene in Coal Produced from Sewage Treatment Station Sludge

Natiele Kleemann [1], Débora Jaeschke [1], Nauro Silveira, Jr. [1], Luiz Pinto [1,*], Tito Cadaval, Jr. [1,*], Jean Arias [1], Sergiane Barbosa [1], Ednei Primel [1] and Adilson Bamberg [2]

[1] Chemistry and Food School, Federal University of Rio Grande–FURG, Rio Grande 96201-90, Brazil; natielekleemannn@gmail.com (N.K.); debora_jaeschke@hotmail.com (D.J.); nauroeq@yahoo.com.br (N.S.J.); jeanarias@furg.br (J.A.); sergianecaldas@furg.br (S.B.); eprimelfurg@gmail.com (E.P.)

[2] Brazilian Agricultural Research Corporation (Embrapa), Pelotas 96010-971, Brazil; adilson.bamberg@embrapa.br

* Correspondence: dqmpinto@furg.br (L.P.); titoeq@gmail.com (T.C.J.)

Abstract: This work investigates the adsorption of benzo[a]pyrene (BaP) using a charcoal adsorbent derived from sewage treatment plant sludge. BaP is a polycyclic aromatic hydrocarbon (PAH), carcinogenic to humans, which his used by the World Health Organization as a marker for all PAH mixtures. The charcoal was produced by the pyrolysis (500 °C, 4 h) of municipal sewage sludge. The resulting biochar presented mesoporous and oxygenated functional groups that are beneficial for the adsorption of benzo[a]pyrene. The material contained graphitic structures, suggesting potential sites for π–π interactions. The adsorption followed the Elovich kinetic model. A maximum adsorbed value of 60.8 μg g^{-1} was achieved for an initial BaP concentration of 100 μg L^{-1} of BaP at 298 K after 20 min. Parameters related to mass transfer phenomena, such as the intraparticle diffusion coefficient, were determined using the homogeneous solid diffusion model (HSDM). These experimental data demonstrate the great potential for computational fluid dynamics (CFD) applications. The value reached for the intraparticle diffusion coefficient was 1.63×10^{-13} m^2s^{-1}. Adsorption equilibrium experiments showed that the Langmuir model was most suitable for experimental data, suggesting a monolayer molecular adsorption process. The results showed that charcoal can be employed as an effective material for removing BaP.

Keywords: polycyclic aromatic hydrocarbon; adsorption; biochar; homogeneous solid diffusion model; environmental remediation

check for updates

Academic Editor: D. Andrew S. Rees

Received: 17 December 2024
Revised: 22 March 2025
Accepted: 27 March 2025
Published: 7 April 2025

Citation: Kleemann, N.; Jaeschke, D.; Silveira, N., Jr.; Pinto, L.; Cadaval, T., Jr.; Arias, J.; Barbosa, S.; Primel, E.; Bamberg, A. Evaluation of the Adsorption Potential of Benzo(a)pyrene in Coal Produced from Sewage Treatment Station Sludge. *Fluids* **2025**, *10*, 98. https://doi.org/10.3390/fluids10040098

Copyright: © 2025 by the authors. Licensee MDPI, Basel, Switzerland. This article is an open access article distributed under the terms and conditions of the Creative Commons Attribution (CC BY) license (https://creativecommons.org/licenses/by/4.0/).

1. Introduction

Emerging contaminants (EC) are chemical compounds of synthetic or natural origin recently identified due to analytical advances. These compounds pose a potential risk to humans and the environment as they exert toxic effects and are bioaccumulative [1,2]. Polycyclic aromatic hydrocarbons (PAHs) belong to the EC group and consist of organic compounds with two or more fused benzene rings. They are commonly found in the environment due to the incomplete combustion of organic matter at high temperatures and low oxygen levels [3]. PAHs are persistent organic pollutants (POPs), and due to their carcinogenicity and widespread presence in the environment, they have raised significant concern in recent years [4,5].

Current studies have shown that PAHs exist in all environments, including water, the atmosphere, soils, and even microorganisms found in polar regions [6]. Some studies have also highlighted the widespread contamination of PAHs in water and soil [7,8]. Adsorption

is a widely studied operation for remediating PAHs' environmental contamination [9] as it is simple, has a low operational cost, and is easy to scale up [10]. In general, the main operational cost is associated with the adsorbent. Therefore, the adsorbent cost must be low to be viable operation on a large scale, such as in soil treatment and ample water sources. This raw material for coal production must be available in abundance. In this context, the sludge generated in sewage treatment plants is widely available and can be used in the pyrolysis reaction.

Sewage treatment plant sludge (STP) is generated from microbial biomass that settles during raw sewage treatment [11]. This sludge is rich in organic matter and nutrients but may contain metals, persistent organic compounds, and pathogens in concentrations harmful to health and the environment [12]. Due to its high temperatures, the pyrolysis reaction can eliminate microbiological and persistent contaminants [13]. Charcoal production from STP is a promising alternative for reducing solid waste and adding value to a material currently a liability for society [14].

To widely use charcoal produced from sewage treatment sludge in PAH environmental adsorption, it is necessary to determine its properties and elucidate its behavior as an adsorbent. Thus, this work aimed to produce charcoal from the sludge generated in a sewage treatment plant, characterize it, and subsequently test it as an adsorbent. The adsorbate chosen was benzo(a)pyrene. The World Health Organization uses benzo(a)pyrene (BaP) as a marker for all PAH mixtures, regardless of composition [15,16]. BaP is a five-ring PAH ubiquitous in the environment, mainly due to emissions from incomplete combustion of organic matter. It is relatively insoluble in water, has low volatility, and is highly lipophilic and stable, accumulating in the body as exposed [17,18]. These characteristics contribute to its environmental persistence and potential for bioaccumulation in living organisms [19].

Although many studies involving PAH adsorption can be found, the information needed to design large-scale unit operations is still scarce. This work aims to elucidate the adsorption phenomena regarding their kinetic, equilibrium and thermodynamic behavior for the SSC-BaP system. This information is essential for industrial unit design, capable of processing large materials amounts. In addition, results of this nature are necessary so that new mathematical approaches can be used, such as computational fluid dynamics (CFD). This tool allows for a more in-depth evaluation of the heat and mass transfer phenomena in adsorption, enabling more outstanding technological advances in developing materials and equipment.

2. Materials and Methods

2.1. Material

The standard solution with BaP at 2000 μg mL^{-1} (molecular formula $C_{20}H_{12}$, molecular weight 252.3 g mol^{-1}) was purchased from Supelco (USA). The optimized three-dimensional structural formula of the BaP (obtained from Molview 2.4 software) is shown in Figure 1. The deuterated PAH (perylene-d12) in a concentration of 4 mg mL^{-1} was purchased from AccuStandard (USA). A 100 mg L^{-1} intermediate standard was prepared using toluene as solvent. Working standard solutions were prepared daily by diluting proper amounts of the PAH mixture in hexane. All solutions were stored in amber glass flasks at −18 °C in the dark. Magnesium sulfate (purity 99.8%) and hexane HPLC grade were purchased from J.T Baker (Mallinckrodt, NJ, USA). The sewage treatment sludge samples were obtained from the wastewater treatment plant in the city of Passo Fundo, Rio Grande do Sul, Brazil (28°15′40″ S, 52°24′30″ W).

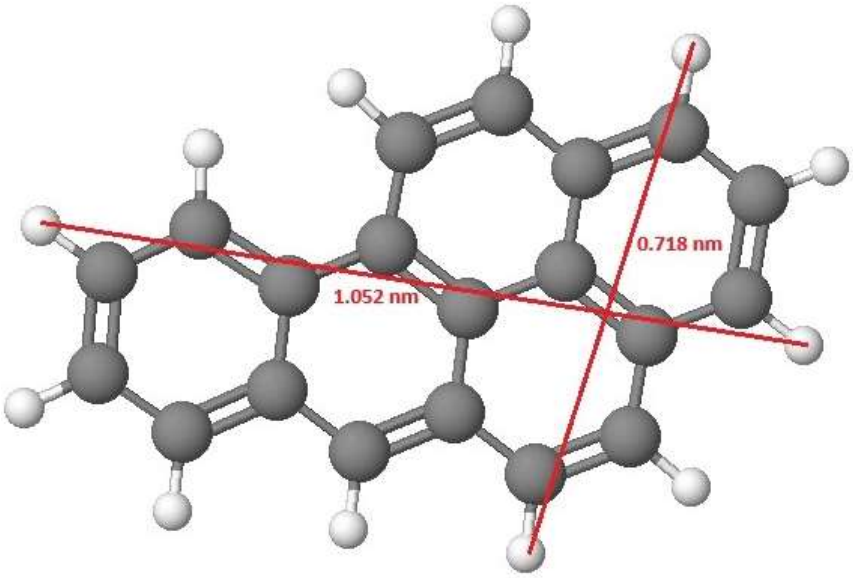


Figure 1. Optimized three-dimensional structural formula of Benzo(a)pyrene (BaP).

2.2. Coal Production

Sewage sludge from a municipal waste treatment plant in Passo Fundo, Brazil, was dried and subjected to pyrolysis in a pilot scale reactor with a capacity of 40 kg per batch. Reaction took place in an inert atmosphere and temperature of 500 °C to produce the sewage sludge coal (SSC). This condition was defined from preliminary tests and, at 500 °C, produced SSC in a pilot reactor presenting similar properties to that produced on a bench scale and avoid PAHs formation.

2.3. Coal Characterization

The SSC samples were characterized regarding their surface properties, including total pore volume, average pore size, specific surface area, and pore size distribution. The total pore volume and average pore size were determined based on nitrogen adsorption/desorption isotherms at 77 K, using an automated gas sorption analyzer. The specific surface area was obtained by the Brunauer–Emmett–Teller (BET) method, while the pore size distribution was obtained by the Barrett–Joyner–Halenda (BJH) method (Micromeritics, Gemini VII 2390, Japan). To evaluate the surface characteristics of the SSCs, scanning electron microscopy (SEM) (model JSM, JEOL, Japan) and energy dispersive spectroscopy (EDS) (model JSM-5800, JEOL, Japan) were used to identify the elemental composition. SSC samples were also characterized by Fourier transform infrared spectroscopy (FTIR) (Prestige, 21210045, Japan), which was performed with total attenuated reflectance (ATR) from 4500 to 450 cm^{-1}.

2.4. Kinetic Experiments and Mass Transfer Mechanism

The kinetic experiments for the adsorption of BaP were carried out using a dosage of 1.0 g L^{-1} of SSC, within an initial total concentration of the BaP of 100 μg L^{-1}. The stirring rate was set to 150 rpm using an orbital shaker, and the temperature was maintained at 25 ± 1 °C. Samples were collected and promptly filtered through filter paper at different times (0, 2, 4, 6, 8, 10, 15, 20, 25, and 30 min). Subsequently, the quantification of BaP was performed following the procedure outlined in Section 2.7. After chromatographic determination, the adsorption capacity at any time (q_t, mg g^{-1}) was calculated using the

pseudo-first-order (PFO), pseudo-second-order (PSO), and Elovich models, expressed by Equations (1), (2), and (3), respectively.

$$q_t = (C_0 - C_t)\frac{V}{m} \tag{1}$$

$$q_t = \frac{t}{(1/k_2 q_2^2) + (t/q_2)} \tag{2}$$

$$q_t = \frac{1}{a}\ln(1 + \text{abt}) \tag{3}$$

where q_t is the amount of adsorbate adsorbed at time t (μg g^{-1}), C_0 is the initial concentration of the adsorbate in the liquid phase (μg L^{-1}), C_t is the concentration of the adsorbate in the liquid phase at any time (μg L^{-1}), m is the mass of adsorbent (g), V is the volume of solution (L), k_2 is the rate constant of pseudo-second order model in (g μg^{-1} min^{-1}), q_2 is the theoretical value for the adsorption capacity (mg g^{-1}), a is the initial adsorption rate (mg g min^{-1}), and b is the desorption constant (mg min^{-1}).

Mass transfer in the adsorption operation occurs at the solid–fluid interface. Therefore, it is correct to state that this phenomenon is affected by both solid and fluid phase diffusion. Gradient concentration effect in liquid phase (fluid phase in this case) can be disregarded due to mechanical mixing. Thus, the adsorbate concentration in the liquid phase can be treated as a function of time only and not as a function of position. Thus, according to Suzuki [20] and Sonetaka et al. [21], external mass transfer can be represented by Equation (4).

$$\frac{dq_t}{dt} = \frac{k_f A}{m}(C_t - C_{st}) \tag{4}$$

where C_{st} (μg L^{-1}) represents the adsorbate concentration on the solid surface, A (m^2) is the adorbent surface area, and k_f (m $s{-}1$) is the external mass transfer coefficient. Substituting Equation (1) into Equation (4), we obtain the following.

$$\frac{dC_t}{dt} = \frac{k_f A}{V}(C_t - C_{st}) \tag{5}$$

Integrating Equation (5) and considering that when $t \to 0$, $C_{st} \to 0$ and $C_t \to C_0$, we obtain [22] the following.

$$ln\left(\frac{C_t}{C_0}\right) = -\frac{k_f A}{V}t \tag{6}$$

Intraparticle diffusivity is a more complex phenomenon and takes into account different factors, making the development of models for these systems a very challenging task. Therefore, the most used model for this purpose is known as homogeneous solid diffusion model (HSDM). In this model, the adsorbent is considered a spherical, amorphous and homogeneous particle and the mass transfer is considered unidirectional and isothermal [20,21,23]. HSDM model is shown in Equation (7).

$$\frac{\partial q}{\partial t} = \left(\frac{1}{r^2}\right)\frac{\partial}{\partial r}\left(r^2 D_i \frac{\partial q}{\partial r}\right) \tag{7}$$

where D_i (m^2 s^{-1}) is the intraparticle diffusion, and r (m) is the radial coordinate. If D_i is considered constant [21,24], the following applies.

$$\frac{\partial q}{\partial t} = D_i\left(\frac{\partial^2 q}{\partial r^2} + \frac{2}{r}\frac{\partial q}{\partial r}\right) \tag{8}$$

Taking $q(r,0) = 0$ as the initial condition and $q(R_p,t) = q_e$ and $(\partial q/\partial r)_{r=0} = 0$ as the boundary conditions.

Under the conditions posed, and for a Fourier number greater than 0.2, Crank (1975) [25] solved the model. This solution can be reduced to the first term of the series, obtaining Equation (9) [20].

$$\frac{q}{q_e} = 1 - \left[\frac{6\alpha(\alpha+1)exp\left(-q_n^2 D_i t/R_p^2\right)}{9+9\alpha+q_n^2\alpha^2}\right] \tag{9}$$

where q_n values are the non-zero roots of Equation (10) as follows.

$$\tan q_n = \frac{3q_n}{3+\alpha q_n^2} \tag{10}$$

2.5. Equilibrium Experiments

The adsorption equilibrium experiment was carried out in a thermostated stirrer (FANEM, 315, SE, Brazil). Flasks containing 100 mL of ultrapure water spiked with 100 µg L^{-1} of BaP were prepared, and SSC was added at different dosages of 0.1, 0.5, 1, 2, 3, 4, and 5 g L^{-1}. The solutions were stirred at 150 rpm for a period of 24 h at 25, 35, 45, and 55 °C to construct the isotherms. Afterwards, the solutions were filtered through filter paper, the PAHs were extracted by salting-out-induced liquid–liquid microextraction (SILLME) and quantified by GC-MS/MS, as described in detail in Section 2.7.

The adsorption capacity at equilibrium (q_e) was determined using Equation (11).

$$q_e = \left(\frac{C_0 - C_e}{m}\right)V \tag{11}$$

where C_e is the equilibrium concentration (µg L^{-1}). The Langmuir and Freundlich isotherm models were used to establish the correlation of the equilibrium curves, according to Equations (12), and (13), respectively.

$$q_e = \frac{q_m k_L C_e}{1+k_L C_e} \tag{12}$$

$$q_e = k_F C_e^{1/n} \tag{13}$$

where q_m is the saturated adsorption capacity (µg g^{-1}), k_L is related to the affinity of the adsorbate for the adsorbent (L mg^{-1}), k_F is the Freundlich constant ((µg g^{-1})(µg L^{-1})$^{-1/n}$), and 1/n is the heterogeneity factor.

2.6. Adsorption Thermodynamics

The thermodynamic parameters, namely, Gibbs free energy (ΔG, kJ mol^{-1}), enthalpy of adsorption (ΔH, kJ mol^{-1}), and entropy of adsorption (ΔS, kJ mol^{-1} K^{-1}) were evaluated. These values indicate the spontaneity of the reaction and the way in which the thermal energy exchange occurs and inform about the energetic heterogeneity of the adsorbent surface. Gibbs free energy can be calculated by Equation (14), where K_D is the thermodynamic equilibrium constant (L mol^{-1}), T is the temperature (K), and R is the universal gas constant (8.314 J mol^{-1} K^{-1}). The K_D values were estimated from the parameters of the best-fit isotherm model [26].

$$\Delta G = -RT\ln K_D \tag{14}$$

The thermodynamic parameters ΔH and ΔS were determined by the Van't Hoff equation (Equation (15)).

$$\ln K_D = \frac{-\Delta H}{RT} + \frac{\Delta S}{R} \quad (15)$$

2.7. BaP Determination

BaP was extracted from SSC samples using the SILLME technique, adapted from Oliveira Arias et al. [27]. For this, 5 mL of the sample and 1 mL of hexane were vortexed for 1 min. Then, 2 g of $MgSO_4$ were added to the mixture, which was agitated again, followed by centrifugation for 5 min at 7793 rpm. Finally, 700 µL of the upper hexane layer was transferred to a GC vial, 35 µL of deuterated internal standard mix was added, and the extract was ready to be injected into the chromatographic system. All analyses were performed in triplicate.

BaP determination was carried out using a gas chromatograph tandem mass spectrometry (model TQ 8050, Shimadzu) equipped with a Combipal AOC 6000 autosampler and a triple quadrupole mass spectrometer detector. A capillary column Rtx®-5MS (30 m × 0.25 mm × 0.25 µm) was used (Restek, Bellefonte, PA, USA). Helium (99.999% purity) was used as a carrier gas at constant flow rate of 1.35 mL min^{-1}. The electron impact (EI) ionization mode was used with a collision energy of 70 eV. The injection volume was 2 µL, the injector temperature was 280 °C, and the in the spitless mode was 150 kPa. The initial oven temperature was 60 °C and held for 1 min. It was then increased to 310 °C at 5 °C min^{-1} and was kept at this temperature for 10 min, resulting in a total analysis time of 61 min. The interface temperature was set at 290 °C, and the ion source temperature was 250 °C.

Compounds were monitored using the selective ion monitoring (SIM) mode. Data acquisition and treatment were performed by the software GCMS solution (version 4.45 SP1, Shimadzu, Japan). The retention times of the monitored ions were compared to those available in a previous study [28].

2.8. Data Analysis

The kinetic and equilibrium parameters were estimated by nonlinear regression using the software Statistica 7.0 (Statsoft, USA). The objective function was quasi–Newton, and the fit quality was evaluated by the coefficient of determination (R^2) and the average relative error (*ARE*). *ARE* calculation was performed according to Equation (16), where $q_{t,exp}$ and $q_{t,pre}$ are the experimental and theoretical adsorption capacity values.

$$ARE = \frac{100}{n}\sum\left|\frac{q_{t,exp} - q_{t,pre}}{q_{t,exp}}\right| \quad (16)$$

3. Results

3.1. Coal Characterization

The charcoal samples were characterized for their total pore volume, average pore size, specific surface area, and pore size distribution. The average pore diameter was 113.21 Å, indicating that the material is mesoporous, type III, according to the IUPAC classification [27]. This result suggests that the SSC produced in this work is adequate for BaP adsorption due to the presence of mesopores. The obtained values for the total pore volume and for the specific surface area were 0.021 cm^3 g^{-1} and 17.68 m^2 g^{-1}, respectively. Similar findings were reported by Zielińska et al. [28], who produced charcoal from sewage sludge for pyrene adsorption. The researchers showed that pyrene, a molecule similar in size to BaP, filled the mesopores, and found a similar value for the specific surface area (18.13 m^2 g^{-1}). Most studies that use charcoal produced from biomass obtain a higher

surface area [29,30]. However, these results are a consequence of the chemical activation of the material, which is commonly applied to increase the surface area. Figure 2 presents the adsorption and desorption isotherms for sewage sludge coal. These isotherms are type IVa with hysteresis loop type H3, indicating that the material is mesoporous and corroborating previous findings [31].

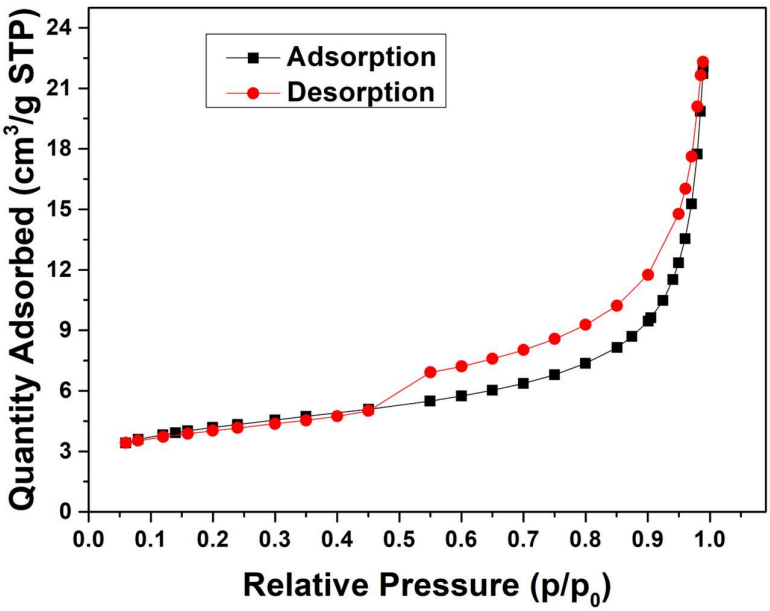


Figure 2. Nitrogen adsorption and desorption isotherms obtained by the Brunauer–Emmett–Teller (BET) method.

Figure 3 shows the SEM images of SSC at 400× (Figure 3A) and 1000× (Figure 3B). The surface morphology appears heterogenous with pores of varying sizes. It is possible to identify some well-defined pores and others with fibrous and rough structures, as well as the presence of ash, tar and other non-volatile compounds. It is important to mention that cylindrical structures with longitudinal pores are a favorable characteristic for the adsorption of BaP in the coal. These structures are a consequence of the precursor material decomposition as no chemical treatment was performed to activate the charcoal in the present study [32].

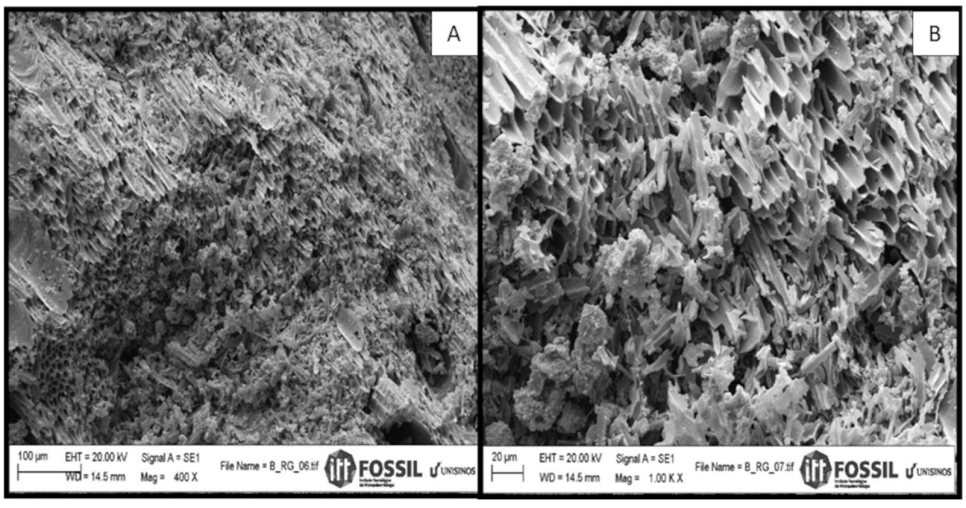


Figure 3. SEM images of sewage sludge charcoal at magnifications of (**A**) 400× and (**B**) 1000×.

Moreover, the images presented in Figure 3 demonstrate that the surface has low porosity. Similar images were presented by Shah et al. [33], which also characterized a biochar obtained from sewage sludge. This heterogeneity of the sample surface is clearly observed in Figure 4, in which some points were selected for qualitative elemental analysis through EDS. It was possible to observe significant variations in the proportion (%, w/w) of some elements at different surface points. At all points, C, O, Fe, Si, Ca, Mg, Al, P, K, and Ti were found. At point 1, which corresponds to the largest area, 33.2% of O, 25.2% of C, 13.2% of Fe, 7.2% of Si, 5.9% of Ca, 5.4% of N, and 4.1% of P were identified, along with minor amounts of Na, Al, K, Mg, and Ti. The mass fraction of C and O was lower at points 2, 3, and 4. For Fe and P, points 2 and 3 presented higher concentrations, reaching 38% of Fe. Si was identified in smaller amounts in points 2 and 3 and in a greater amount at point 4. N was not identified at points 2, 3, and 4. This result also highlights the absence of heavy metals on the biochar surface. This type of contaminant is a source of great concern when charcoal is produced from sewage sludge treatment since they are not eliminated by thermal pyrolysis treatment, as occurs through microbiological contamination.

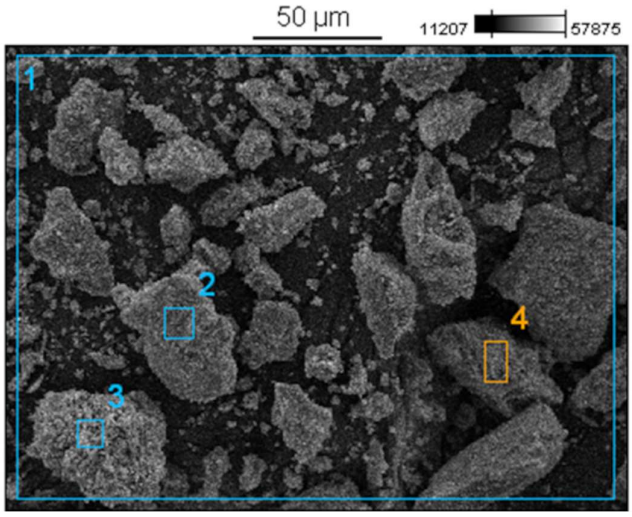


Figure 4. SEM images of sewage sludge coal. The points 1, 2, 3, and 4 were selected to evaluate the chemical composition of the material by EDS analysis.

The large amount of carbon may indicate that the biochar structure is aromatic and may result in π–π interactions with aromatic groups in organic pollutants [34]. Regarding oxygen, a large amount of this element is possibly presented in the material in the form of oxides combined with other elements detected in the spectrum, such as Si, Al, Mg, Ca, and Fe. These oxides are important in the adsorption process of organic substances in aqueous solutions as they facilitate interaction with the adsorbent. Silicon corresponds to approximately 6% of the material mass. The presence of this element was expected since sludge contains large amounts of clay, silt, and sand. Calcium was also detected, and its presence is possibly due to the addition of lime, in the form of a $Ca(OH)_2$ suspension during the sludge treatment. The presence of Fe and Al may be due to the use of iron-based and aluminum sulfate anticoagulants in sewage treatment. Moreover, small amounts of other elements were also detected, possibly because they remain attached to the carbon structure in the precursor material, located on the surface of the ring blades [32].

3.2. Kinetics Experiments and Mass Transfer Mechanism

Initially, before carrying out the adsorption experiments, tests were carried out to verify whether any compound would be released by the SSC, and no release of any compound by the adsorbent was detected.

Figure 5 presents the amount of BaP adsorbed over time (0 to 30 min). The kinetic analysis was carried out using BaP (100 μg L^{-1}) and SSC (1 mg L^{-1}) at 298 K and a stirring rate of 150 rpm. It is possible to observe that the maximum adsorption was 60.81 μg L^{-1}, achieved after 20 min of the process. To explain the adsorption kinetics, the experimental data were fitted to PFO, PSO, and the Elovich models. The outcomes of this analysis are presented in Table 1, and the kinetic curves are presented in Figure 5. The results revealed that the Elovich model was the most suitable for representing the experimental kinetic data, presenting higher R^2 value (≥0.9) and lower ARE (<10%). The Elovich model characterizes the chemisorption process on heterogeneous surfaces [35]. According to this model, the rate of adsorption depends on the amount of solute adsorbed on the adsorbent's surface and the amount adsorbed at equilibrium. It also indicates that the rate decreases over time due to increased surface coverage as chemisorption is an irreversible process [36].

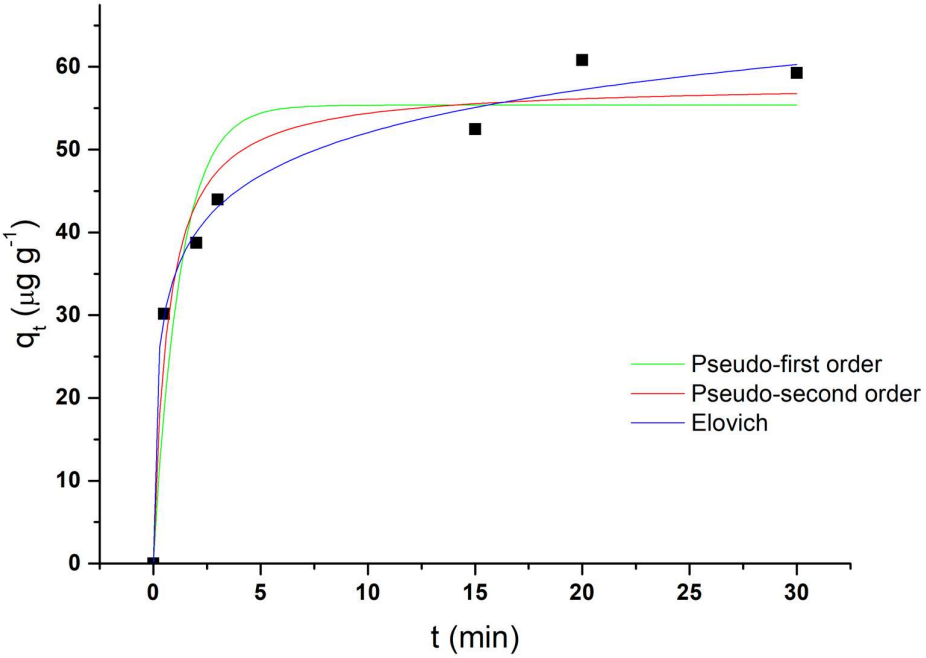


Figure 5. Adsorption kinetics for benzo[a]pyrene on sewage sludge coal at 298 K. The points represent experimental data and lines represent the pseudo-first-order, pseudo-second-order, and Elovich models.

Table 1. Parameters of adsorption kinetic for benzo[a]pyrene.

Elovich	**a (g μg^{-1})**	**b (μg g^{-1} min^{-1})**	**R^2**	**ARE (%)**
	0.16	1478	0.90	8.43
Pseudo-First Order	q_1 (μg g^{-1})	k_1 (min^{-1})	R^2	ARE (%)
	47.11	1.85	0.77	13.20
Pseudo-Second Order	q_2 (μg g^{-1})	k_2 (g μg^{-1} min^{-1})	R^2	ARE (%)
	51.40	0.04	0.83	12.44

Chemical interactions also govern the adsorption process in this study through the sharing or exchange of electrons between the adsorbate and the adsorbent [37]. As observed in the sample characterization analyses, the presence of functional groups allows for greater adsorption of the molecules on the adsorbent. The most likely adsorption mechanisms occurred through π–π interaction, pore filling, hydrophobic interactions, and hydrogen bonds between PAHs and biochar [38].

Using kinetic information was possible to determine external and intraparticle mass transfer parameters, as shown in Table 2. To determine kf, the first points of the kinetic curve

were used, which present the linear behavior represented by Equation (6). Results show good agreement with experimental data (>0.9) and a relatively small error (ARE < 2%). To determine the intraparticle diffusion coefficient (Di), the first points of the kinetic curve were excluded. This was undertaken because the model used considers that the concentration on the particle adsorbent surface in R_p is saturated. This consideration is quite far from reality when $t \to 0$. Under this consideration, the model for intraparticle mass transfer also showed good correlation with the experimental results, and ARE indicates good data prediction.

Table 2. Mass transfer parameters for BaP in biochar.

k_f (m s^{-1})		D_i (m^2 s^{-1})	
Value $\times 10^4$	2.15	Value $\times 10^{13}$	1.31
R^2	0.93	R^2	0.92
ARE (%)	1.73	ARE (%)	5.94

Although these models can be used for many applications, they have the limitation of not being extrapolated to other operational conditions such as prediction at other temperatures or other mechanical mixing conditions. These parameters will only present good results if the process conditions are approximately the same as the experimental ones. Thus, CFD (computational fluid dynamics) tools can present more promising ways of modeling adsorption operations, allowing us to understand the phenomena involved in this operation more deeply and to develop more comprehensive models.

3.3. Isotherms and Thermodynamics

Figure 6 shows the experimental data of BaP adsorption onto SSC adjusted by equilibrium models. The results show that higher temperatures lead to increased adsorption capacities, with maximum values ranging from 58 to 114.52 μg L^{-1}. To determine the most suitable correlation for the equilibrium curves and estimate the isotherm parameters, two mathematic models, Langmuir and Freundlich, were applied to the experimental data. Table 3 provides the isotherm parameters obtained for all the temperatures studied.

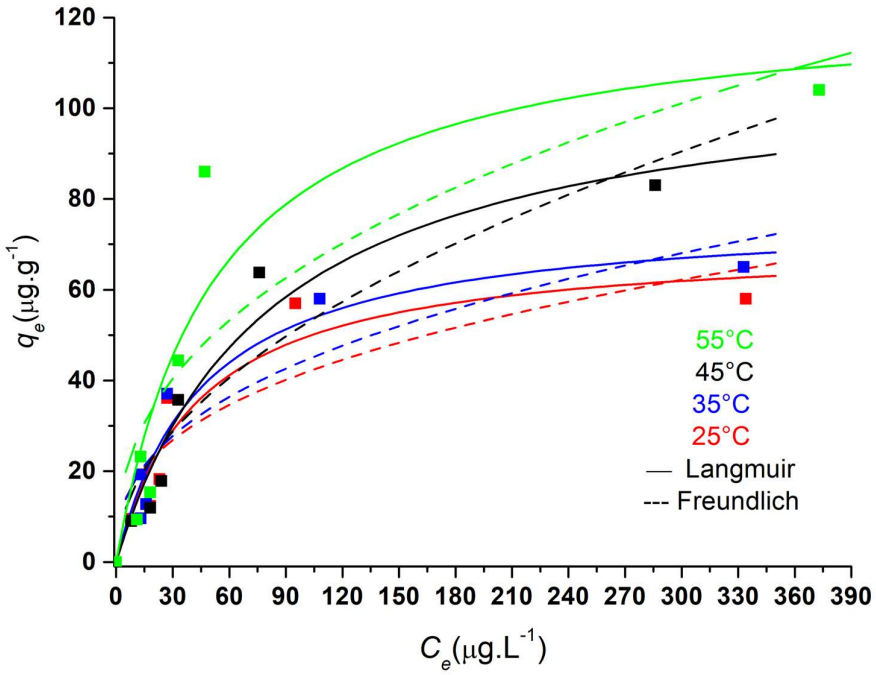


Figure 6. Isotherm models of adsorption capacity of benzo[a]pyrene by sewage sludge coal.

Table 3. Isotherm parameters for benzo[a]pyrene adsorption onto sewage sludge coal.

	Temperature (°C)			
	25 °C	**35 °C**	**45 °C**	**55 °C**
Langmuir				
$\mathbf{q_m}$ (μg g^{-1})	70.840	77.030	110.430	124.311
k_L	0.023	0.022	0.012	0.019
$\mathbf{R^2}$	0.9128	0.9452	0.9564	0.8755
ARE (%)	23.9	25.82	21.82	39.8
Freundlich				
k_F	7.786	7.401	5.295	10.429
N	2.745	2.570	2.009	2.509
$\mathbf{R^2}$	0.8176	0.8716	0.8976	0.7799
ARE (%)	36.79	34.57	35.23	53.89

The results in Table 3 show that the Langmuir model presented higher R^2 and lower ARE values, indicating that this model provided the best fit to the experimental equilibrium data in all of the conditions studied. Other authors also found that the Langmuir model was the most suitable one for the adsorption of Cr (VI) using biochar from sewage sludge [39]. As to the maximum adsorption capacity (q_m), it increased with temperature, reaching a maximum value of 124.3 μg g^{-1} at 55 °C. These findings suggested that BaP adsorption was a monolayer molecular adsorption process and that chemisorption was involved. The chemisorption process may be related to the abundant functional groups on the SSC samples. These results were corroborated by the FTIR analysis, which suggested the presence of π–π EDA interactions, indicating adsorption mechanism. The aromatic structure of BaP could serve as an electron donor for π–π EDA interactions with the electron-deficient aromatic structures on the surface of SSC [40].

The thermodynamic adsorption characteristics of BaP by SSC were assessed by calculating the enthalpy, entropy, and Gibbs free energy changes, and the results are presented in Table 4. The enthalpy change in the process was calculated by Arrhenius equation using the K_D values derived from the Langmuir parameters with the adjusted data presented in Figure 7. The negative ΔG values indicated that the BaP adsorption by SSC was a spontaneous and favorable process. The values ranging from −15.84 to −20.44 indicated that the spontaneity increased with the increase in temperature. The positive ΔH value show that the adsorption process was endothermic, and the positive ΔS value indicated that the disorder in the solid–liquid interface increased during the adsorption process.

Table 4. Thermodynamic parameters for the benzo[a]pyrene adsorption.

T (°C)	$\mathbf{K_D}$	**ΔG (kJmol^{-1})**	**ΔS (J·mol^{-1}K^{-1})**	**ΔH (kJmol^{-1})**
25	598.23	−15.84	151.98	30.04
35	533.83	−16.80		
45	831.25	−17.77		
55	1803.60	−20.44		

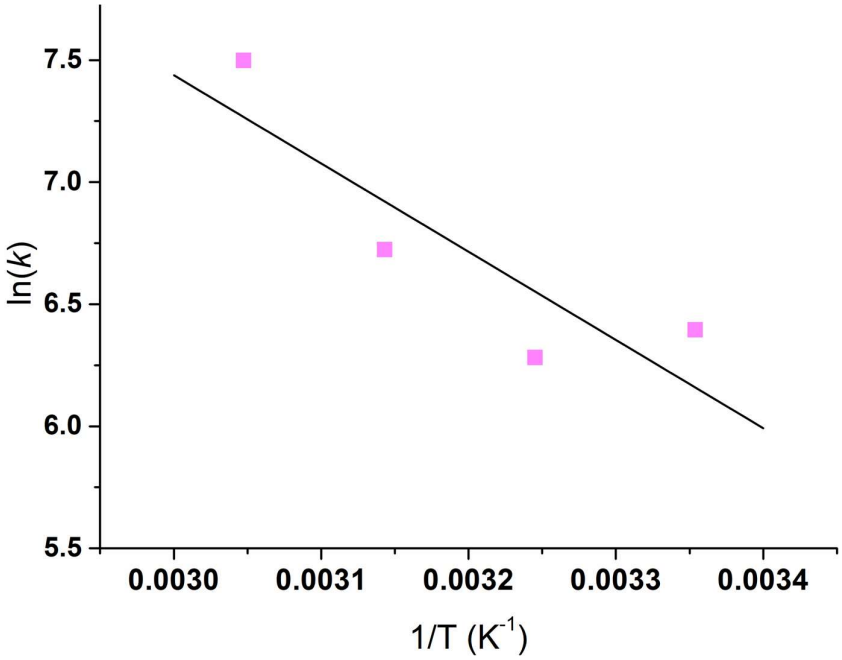


Figure 7. Thermodynamic adsorption of benzo[a]pyrene by sewage sludge coal.

After achieving results for kinetic and equilibrium experiments, it is possible to verify that the SSC has a moderate adsorption capacity compared to high-performance adsorbents. This can be attributed to the low initial concentration of the adsorbate since this research tried to use concentrations similar to the real effluent. Moreover, it is essential to emphasize that the sludge used as a raw material for charcoal production is available in great abundance, and its natural state represents a problem for society due to the possibility of microbiological contamination. Thus, transforming this material into biochar can represent a solution for communities and environmental remediation processes when large quantities of adsorbent are needed. The matrix effect can affect adsorption operations in real and complex systems, which is generated by competing other compounds for the adsorption sites on the solid surface. However, it is necessary to know the adsorption mechanism to elucidate the adsorption phenomenon. This adsorbent–adsorbate interaction can only be elucidated using a model system.

4. Conclusions

This study focused on exploring the utilization of sewage sludge coal to remove benzo[a]pyrene from aqueous solutions by adsorption. The charcoal was produced by pyrolysis from sewage sludge at 500 °C for 4 h, yielding a material with satisfactory properties. Since sludge is available in large quantities, this highlights its potential for large-scale charcoal production. Furthermore, the pyrolysis heat treatment ensures the elimination of pathogenic biological contaminants. In preliminary texts, the adsorbent did not release any toxic compounds, showing that the sludge obtained from this station can be used. The characterization analysis suggested that interactions between BaP and SSC occurred by pore filling and π–π EDA interactions. Experimental results could be satisfactorily correlated by mathematical models, evidencing a regular behavior of the SSC-BaP system. The Elovich model presented adequate fit with the experimental kinetic data ($R^2 > 0.90$ and ARE < 9.00). The Langmuir model was the most adequate to represent the equilibrium adsorption isotherms as it presented higher R^2 and lower ARE than the Freundlich model. The maximum adsorption capacity was 124.3 μg g^{-1} obtained at 55 °C. The negative values of ΔG and positive values of ΔH showed that the BaP

adsorption by SSC was a spontaneous favorable and endothermic process. The reasonable adjustment of models to experimental data provides an essential tool for process and equipment design. Due to the complexity of adsorption studies, the search for more comprehensive phenomenological models remains a significant challenge. Tools like CFD can solve complex mathematical models developed to correlate this information, proposing a paradigm shift in the modeling of adsorption processes.

Author Contributions: N.K., conceptualization, methodology, validation, formal analysis, investigation, data curation, writing—original draft, methodology, validation, formal analysis; D.J., writing—review, methodology, validation, formal analysis; N.S.J., conceptualization, writing—review, methodology, validation, formal analysis; L.P., resources, writing—review and editing, supervision; T.C.J., writing—review and editing, supervision, project administration; J.A., methodology, validation, formal analysis, data curation; S.B., writing—review and editing, supervision, project administration; E.P., writing—review and editing, supervision, project administration; A.B., writing—review and editing, supervision, project administration. All authors have read and agreed to the published version of the manuscript.

Funding: Part of this study was funded by the Coordenação de Aperfeiçoamento de Pessoal de Nível Superior—Brasil (CAPES)—Finance Code 001. E.G. Primel received a productivity research fellowship from the Brazilian Agency CNPq (DT 305716/2020-4).

Data Availability Statement: The raw data supporting the conclusions of this article will be made available by the authors on request.

Acknowledgments: The authors acknowledge the financial support provided by the Brazilian agencies FAPERGS (21/2551-0000684-6), CNPq, and FINEP. Part of this study was funded by the Coordenação de Aperfeiçoamento de Pessoal de Nível Superior—Brasil (CAPES)—Finance Code 001. E.G. Primel received a productivity research fellowship from the Brazilian Agency CNPq (DT 305716/2020-4). The authors are thankful to the Integrated Analysis Center (CIA), the Center for Electron Microscopy of the South Zone CEME-SUL. G. L, and the Brazilian Agricultural Research Corporation (Embrapa).

Conflicts of Interest: Author Adilson Bamberg was employed by the company Brazilian Agricultural Research Corporation (Embrapa). The remaining authors declare that the research was conducted in the absence of any commercial or financial relationships that could be construed as a potential conflict of interest.

References

1. Mukhopadhyay, A.; Duttagupta, S.; Mukherjee, A. Emerging Organic Contaminants in Global Community Drinking Water Sources and Supply: A Review of Occurrence, Processes and Remediation. *J. Environ. Chem. Eng.* **2022**, *10*, 107560. [CrossRef]
2. Wang, F.; Xiang, L.; Sze-Yin Leung, K.; Elsner, M.; Zhang, Y.; Guo, Y.; Pan, B.; Sun, H.; An, T.; Ying, G.; et al. Emerging Contaminants: A One Health Perspective. *Innovation* **2024**, *5*, 100612. [PubMed]
3. Sampaio, G.R.; Guizellini, G.M.; da Silva, S.A.; de Almeida, A.P.; Pinaffi-Langley, A.C.C.; Rogero, M.M.; de Camargo, A.C.; Torres, E.A.F.S. Polycyclic Aromatic Hydrocarbons in Foods: Biological Effects, Legislation, Occurrence, Analytical Methods, and Strategies to Reduce Their Formation. *Int. J. Mol. Sci.* **2021**, *22*, 6010. [CrossRef]
4. Song, X.; Li, J.; Xu, S.; Ying, R.; Ma, J.; Liao, C.; Liu, D.; Yu, J.; Chen, L. Determination of 16 Polycyclic Aromatic Hydrocarbons in Seawater Using Molecularly Imprinted Solid-Phase Extraction Coupled with Gas Chromatography-Mass Spectrometry. *Talanta* **2012**, *99*, 75–82. [CrossRef]
5. Vijayanand, M.; Ramakrishnan, A.; Subramanian, R.; Issac, P.K.; Nasr, M.; Khoo, K.S.; Rajagopal, R.; Greff, B.; Wan Azelee, N.I.; Jeon, B.H.; et al. Polyaromatic Hydrocarbons (PAHs) in the Water Environment: A Review on Toxicity, Microbial Biodegradation, Systematic Biological Advancements, and Environmental Fate. *Environ. Res.* **2023**, *227*, 115716. [CrossRef]
6. Wei, L.; Lv, J.; Zuo, P.; Li, Y.; Yang, R.; Zhang, Q.; Jiang, G. The Occurrence and Sources of PAHs, Oxygenated PAHs (OPAHs), and Nitrated PAHs (NPAHs) in Soil and Vegetation from the Antarctic, Arctic, and Tibetan Plateau. *Sci. Total Environ.* **2024**, *912*, 169394. [CrossRef]

7. Guo, M.; Shang, X.; Ma, Y.; Zhang, K.; Zhang, L.; Zhou, Y.; Gong, Z.; Miao, R. Biochars Assisted Phytoremediation of Polycyclic Aromatic Hydrocarbons Contaminated Agricultural Soil: Dynamic Responses of Functional Genes and Microbial Community. *Environ. Pollut.* **2024**, *345*, 123476. [CrossRef]
8. Dong, M.; He, L.; Jiang, M.; Zhu, Y.; Wang, J.; Gustave, W.; Wang, S.; Deng, Y.; Zhang, X.; Wang, Z. Biochar for the Removal of Emerging Pollutants from Aquatic Systems: A Review. *Int. J. Environ. Res. Public Health* **2023**, *20*, 1679. [CrossRef]
9. Pathak, S.; Sakhiya, A.K.; Anand, A.; Pant, K.K.; Kaushal, P. A State-of-the-Art Review of Various Adsorption Media Employed for the Removal of Toxic Polycyclic Aromatic Hydrocarbons (PAHs): An Approach towards a Cleaner Environment. *J. Water Process Eng.* **2022**, *47*, 102674. [CrossRef]
10. Gonçalves, J.O.; de Farias, B.S.; Rios, E.C.; Jaeschke, D.P.; Ribeiro, A.C.; da Silva, M.D.; Vieira, M.L.G.; Carvalho, V.V.D.L.; Cadaval, T.R.S.; Pinto, L.A.D.A. Advances in Chitosan-Based Materials for Application in Catalysis and Adsorption of Emerging Contaminants. *Sustainability* **2024**, *16*, 8321. [CrossRef]
11. Kacprzak, M.; Neczaj, E.; Fijałkowski, K.; Grobelak, A.; Grosser, A.; Worwag, M.; Rorat, A.; Brattebo, H.; Almås, Å.; Singh, B.R. Sewage Sludge Disposal Strategies for Sustainable Development. *Environ. Res.* **2017**, *156*, 39–46. [CrossRef] [PubMed]
12. Ivanová, L.; Mackuľak, T.; Grabic, R.; Golovko, O.; Koba, O.; Staňová, A.V.; Szabová, P.; Grenčíková, A.; Bodík, I. Pharmaceuticals and Illicit Drugs—A New Threat to the Application of Sewage Sludge in Agriculture. *Sci. Total Environ.* **2018**, *634*, 606–615. [CrossRef] [PubMed]
13. Zheng, H.; Liu, B.; Liu, G.; Cai, Z.; Zhang, C. Potential Toxic Compounds in Biochar: Knowledge Gaps Between Biochar Research and Safety. In *Biochar from Biomass and Waste: Fundamentals and Applications*; Elsevier: Amsterdam, The Netherlands, 2019; pp. 349–384. [CrossRef]
14. Dudnikova, T.; Wong, M.H.; Minkina, T.; Sushkova, S.; Bauer, T.; Khroniuk, O.; Barbashev, A.; Shuvaev, E.; Nemtseva, A.; Kravchenko, E. Effects of Pyrolysis Conditions on Sewage Sludge-Biochar Properties and Potential Risks Based on PAH Contents. *Environ. Res.* **2025**, *266*, 120444. [CrossRef]
15. Reizer, E.; Csizmadia, I.G.; Palotás, Á.B.; Viskolcz, B.; Fiser, B. Formation Mechanism of Benzo(a)Pyrene: One of the Most Carcinogenic Polycyclic Aromatic Hydrocarbons (PAH). *Molecules* **2019**, *24*, 1040. [CrossRef]
16. Aquilina, N.J.; Harrison, R.M. Evaluation of the Cancer Risk from PAHs by Inhalation: Are Current Methods Fit for Purpose? *Environ. Int.* **2023**, *177*, 107991. [CrossRef]
17. Speciale, A.; Zena, R.; Calabrò, C.; Bertuccio, C.; Aragona, M.; Saija, A.; Trombetta, D.; Cimino, F.; Lo Cascio, P. Experimental Exposure of Blue Mussels (*Mytilus galloprovincialis*) to High Levels of Benzo[a]Pyrene and Possible Implications for Human Health. *Ecotoxicol. Environ. Saf.* **2018**, *150*, 96–103. [CrossRef]
18. Cao, W.; Luo, Y.; Li, J.; Qian, A.; Wang, Q.; Wang, X.; Duan, L.; Wu, Y.; Han, C. Detection of Benzo[a]Pyrene with Silver Nanorod Substrate in River Water and Soil Based on Surface-Enhanced Raman Scattering. *Results Chem.* **2021**, *3*, 100126. [CrossRef]
19. Bukowska, B.; Mokra, K.; Michałowicz, J. Benzo[a]Pyrene—Environmental Occurrence, Human Exposure, and Mechanisms of Toxicity. *Int. J. Mol. Sci.* **2022**, *23*, 6348. [CrossRef]
20. Suzuki, M. *Adsorption Engineering, Suzuki (1990)*; Elsevier Science Publishers B.V.: Amsterdam, The Netherlands, 1990; ISBN 0-444-98802-5.
21. Sonetaka, N.; Fan, H.J.; Kobayashi, S.; Chang, H.N.; Furuya, E. Simultaneous Determination of Intraparticle Diffusivity and Liquid Film Mass Transfer Coefficient from a Single-Component Adsorption Uptake Curve. *J. Hazard. Mater.* **2009**, *164*, 1447–1451. [CrossRef]
22. Roberts, P.V.; Cornel, P.; Summers, R.S. External Mass-Transfer Rate in Fixed-Bed Adsorption. *J. Environ. Eng.* **1985**, *111*, 891–905. [CrossRef]
23. Helfferich, F.G. Principles of Adsorption & Adsorption Processes, by D. M. Ruthven, John Wiley & Sons, 1984, Xxiv + 433 Pp. *AIChE J.* **1985**, *31*, 523–524. [CrossRef]
24. Qiu, H.; Lv, L.; Pan, B.C.; Zhang, Q.J.; Zhang, W.M.; Zhang, Q.X. Critical Review in Adsorption Kinetic Models. *J. Zhejiang Univ. Sci. A* **2009**, *10*, 716–724. [CrossRef]
25. Crank, J. *The Mathematics of Diffusion*, 2nd ed.; Oxford University Press: Oxford, UK, 1975.
26. Milonjić, S.K. A Consideration of the Correct Calculation of Thermodynamic Parameters of Adsorption. *J. Serbian Chem. Soc.* **2007**, *72*, 1363–1367. [CrossRef]
27. De Oliveira Arias, J.L.; Rocha, C.B.; Kupski, L.; Barbosa, S.C.; Primel, E.G. Salting-Out Induced Liquid-Liquid Microextraction: An Environmentally Friendly Approach to Preservative Determination in Food Samples. *Food Anal. Methods* **2021**, *14*, 1625–1636. [CrossRef]
28. Marcolin, L.C.; de Oliveira Arias, J.L.; Kupski, L.; Barbosa, S.C.; Primel, E.G. Polycyclic Aromatic Hydrocarbons (PAHs) in Honey from Stingless Bees (Meliponinae) in Southern Brazil. *Food Chem.* **2023**, *405*, 134944. [CrossRef]
29. Sing, K.S.W. Characterization Of Porous Solids: An Introductory Survey. In *Studies in Surface Science and Catalysis*; Elsevier: Amsterdam, The Netherlands, 1991; Volume 62, pp. 1–9. [CrossRef]

30. Zielińska, A.; Oleszczuk, P. Evaluation of Sewage Sludge and Slow Pyrolyzed Sewage Sludge-Derived Biochar for Adsorption of Phenanthrene and Pyrene. *Bioresour. Technol.* **2015**, *192*, 618–626. [CrossRef]
31. Melo, J.M.; Lütke, S.F.; Igansi, A.V.; Franco, D.S.P.; Vicenti, J.R.M.; Dotto, G.L.; Pinto, L.A.A.; Cadaval, T.R.S.; Felipe, C.A.S. Mass Transfer and Equilibrium Modelings of Phenol Adsorption on Activated Carbon from Olive Stone. *Colloids Surf. A Physicochem. Eng. Asp.* **2024**, *680*, 132628. [CrossRef]
32. Gonçalves, J.O.; Crispim, M.M.; Rios, E.C.; Silva, L.F.; de Farias, B.S.; Sant'Anna Cadaval Junior, T.R.; de Almeida Pinto, L.A.; Nawaz, A.; Manoharadas, S.; Dotto, G.L. New and Effective Cassava Bagasse-Modified Biochar to Adsorb Food Red 17 and Acid Blue 9 Dyes in a Binary Mixture. *Environ. Sci. Pollut. Res. Int.* **2024**, *31*, 5209–5220. [CrossRef]
33. Thommes, M.; Kaneko, K.; Neimark, A.V.; Olivier, J.P.; Rodriguez-Reinoso, F.; Rouquerol, J.; Sing, K.S.W. Physisorption of Gases, with Special Reference to the Evaluation of Surface Area and Pore Size Distribution (IUPAC Technical Report). *Pure Appl. Chem.* **2015**, *87*, 1051–1069. [CrossRef]
34. Rodríguez-Reinoso, F.; Molina-Sabio, M. Textural and Chemical Characterization of Microporous Carbons. *Adv. Colloid Interface Sci.* **1998**, *76–77*, 271–294. [CrossRef]
35. Shah, A.; Arjunan, A.; Thumma, A.; Zakharova, J.; Bolarinwa, T.; Devi, S.; Batool, M. Adsorptive Removal of Arsenic from Drinking Water Using KOH-Modified Sewage Sludge-Derived Biochar. *Clean. Water* **2024**, *2*, 100022. [CrossRef]
36. Hoslett, J.; Ghazal, H.; Mohamad, N.; Jouhara, H. Removal of Methylene Blue from Aqueous Solutions by Biochar Prepared from the Pyrolysis of Mixed Municipal Discarded Material. *Sci. Total Environ.* **2020**, *714*, 136832. [CrossRef] [PubMed]
37. Wu, F.C.; Tseng, R.L.; Juang, R.S. Characteristics of Elovich Equation Used for the Analysis of Adsorption Kinetics in Dye-Chitosan Systems. *Chem. Eng. J.* **2009**, *150*, 366–373. [CrossRef]
38. Hu, S.; Xu, D.; Kong, X.; Gong, J.; Yang, Y.; Ran, Y.; Mao, J. Effect of the Structure and Micropore of Activated and Oxidized Black Carbon on the Sorption and Desorption of Nonylphenol. *Sci. Total Environ.* **2021**, *761*, 144191. [CrossRef]
39. Liu, S. Cooperative Adsorption on Solid Surfaces. *J. Colloid Interface Sci.* **2015**, *450*, 224–238. [CrossRef]
40. Barman, S.R.; Das, P.; Mukhopadhayay, A. Biochar from Waste Sterculia Foetida and Its Application as Adsorbent for the Treatment of PAH Compounds: Batch and Optimization. *Fuel* **2021**, *306*, 121623. [CrossRef]

Disclaimer/Publisher's Note: The statements, opinions and data contained in all publications are solely those of the individual author(s) and contributor(s) and not of MDPI and/or the editor(s). MDPI and/or the editor(s) disclaim responsibility for any injury to people or property resulting from any ideas, methods, instructions or products referred to in the content.